XLVI CILAMCE
VITÓRIA - ES - BRAZIL - 2025
XLVI IBERO-LATIN AMERICAN CONGRESS ON COMPUTATIONAL METHODS IN ENGINEERING

Thermal analysis of axisymmetric domains using the polar coordinate formulation of the finite-volume theory

Eliedson R. de Carvalho[1], Romildo dos S. Escarpini Filho[2], Márcio A. A. Cavalcante[3]

[1]*Center of Technology, Federal University of Alagoas*
Av. Lourival Melo Mota, Maceió, 57072-900, Alagoas, Brazil
Campus Palmeira dos Índios, Federal Institute of Alagoas
eliedson.carvalho@ctec.ufal.br, eliedson.carvalho@ifal.edu.br
[2]*Campus Arapiraca, Federal University of Alagoas*
Av. Beira Rio - Historic Center, Penedo, 57200-000, Alagoas, Brazil
romildo.escarpini@penedo.ufal.br
[3]*Campus of Engineering and Agricultural Sciences, Federal University of Alagoas*
BR-104 – km 85, Rio Largo, 57100-000, Alagoas, Brazil
marcio.cavalcante@ceca.ufal.br

Abstract. Thermal analysis plays a critical role in engineering, especially when evaluating materials and components under complex operating conditions. In this context, understanding temperature distributions within axisymmetric domains—such as cylindrical structures, pipes, and circular rings—is essential to ensure reliable performance and structural integrity. This work presents a thermal analysis approach for axisymmetric domains based on a polar-coordinate formulation of the Finite-Volume Theory (FVT). The formulation assembles local thermal conductivity matrices using surface-averaged temperatures and heat fluxes evaluated at the interfaces of the discretized subvolumes. Two benchmark problems are analyzed: a homogeneous metallic tube and a functionally graded material (FGM) tube with a ceramic–metal variation across the radius. The global system is constructed by enforcing local energy balance and compatibility conditions between adjacent subvolumes. Numerical results obtained from computational simulations show excellent agreement with analytical solutions, confirming the accuracy and robustness of the proposed formulation. Additionally, the approach proves efficient for axisymmetric problems, as it naturally adapts to curved geometries and does not require discretization in the circumferential direction.

Keywords: axisymmetric domains, computational simulations, finite-volume theory, polar coordinates, thermal analysis.

1 Introduction

The analysis of heat transfer in engineering systems plays a relevant role in the design and performance evaluation of thermal equipment, energy conversion devices, and structural components exposed to temperature gradients. In particular, radial and axisymmetric heat conduction problems are frequently encountered in pipelines, cylindrical walls, and pressure vessels, where the geometry imposes a natural formulation in polar coordinates. Analytical methods, although powerful in specific canonical cases, rapidly become intractable for more complex geometries or boundary conditions, thereby justifying the widespread adoption of numerical techniques.

To analyze temperature distribution in materials, numerical modeling is often preferred over experiments and analytical methods due to its accuracy, lower cost, and adaptability. Experiments are expensive and time-consuming, while analytical solutions are limited by complex equations and boundary conditions, as stated by Santos *et al.* [1]. In this context, the Finite-Volume Theory (FVT) has emerged as a robust and physically consistent numerical tool for solving a variety of engineering problems. The Finite-Volume Theory stems from the reformulated higher-order theory, presented by Bansal and Pindera [2], which simplified discretization and matrix assembly for graded materials. FVT naturally ensures flux balance at the control volume level, satisfying the

compatibility conditions in a surface-average sense, and is particularly suited for thermal analysis of heterogeneous materials, as discussed by Bansal and Pindera [2], Zhong [3], Zhong *et al.* [4] and Cavalcante *et al.* [5-6].

Several developments have extended the classical FVT into generalized formulations capable of treating parametric temperature fields within arbitrarily shaped subvolumes. In this context, Cavalcante et al. [5-6] developed the parametric formulation of the finite-volume theory, introducing polynomial representations of the temperature field within control volumes, enabling the derivation of local conductivity matrices through direct integration of the governing equations. This approach offers a more refined representation of the thermal behavior inside complex geometries while preserving the conservative nature of the method.

The theoretical groundwork laid by Bansal and Pindera [2], and later expanded by Cavalcante *et al.* [5-6], demonstrated the applicability of the parametric finite-volume formulation to both Cartesian and curvilinear grids, paving the way for its use in polar and cylindrical coordinates. More recent efforts have focused on computational optimization and numerical stability, such as the checkerboard-free topological formulations for elastic systems, presented by Araujo *et al.* [7], and the stress analysis in axisymmetric structures using the Finite-Volume Theory formulation in polar coordinates, as discussed by Santos and Cavalcante [8].

Despite recent advances, this work aims to fill this gap by developing and validating a Finite-Volume Theory formulation in polar coordinates for steady-state heat conduction in axisymmetric domains. The local temperature field is represented by second-order polynomials, and energy conservation is enforced over each subvolume using surface-averaged fluxes. Three MATLAB® implementations were developed to assess the temperature field representation, the method's accuracy, and convergence behavior. The proposed approach is evaluated for both homogeneous and functionally graded materials (FGM), with results compared to analytical solutions.

2 Finite-Volume Theory (FVT) formulation in polar coordinates

The Finite-Volume Theory applied in this work aims to extend to thermal analysis the technique presented by Santos and Cavalcante [8]. In FVT formulation in polar coordinates, the subvolume position is determined in terms of radial and circumferential (angular) coordinates. The differential heat conduction equation is satisfied in an average-sense within the volume, and the temperature field in each subvolume is represented by second-order polynomials defined in local polar coordinates. Moreover, the method naturally handles non-Cartesian boundaries and satisfies the compatibility conditions in a surface-average sense.

2.1 Discretization and temperature field representation

Figure 1 presents a circular domain subdivided into $N_s = N_\beta N_\gamma$ curvilinear quadrilateral subdomains referred to as subvolumes. The values N_β and N_γ represent the number of subdivisions corresponding to the intervals $R_I \leq r \leq R_I + E = R_E$ and $0 \leq \theta \leq A$, respectively. Each subvolume can be designated by a single index $1 \leq s \leq N_s$ or by a pair of indexes $\beta = 1, \cdots, N_\beta$ and $\gamma = 1, \cdots, N_\gamma$, where the first is derived from the latter two. For instance, the subvolume (β, γ) is the one occupying the β-th position in the radial direction and the γ-th position in the circumferential direction, or the s-th position in the discretized structure, where $s = \gamma + (\beta - 1)N_\gamma$. Additionally, the heat fluxes and temperatures imposed on the analyzed domain are applied to the outer faces of the subvolumes located on the periphery of the model, considering the surface-averaged values of these thermal quantities.

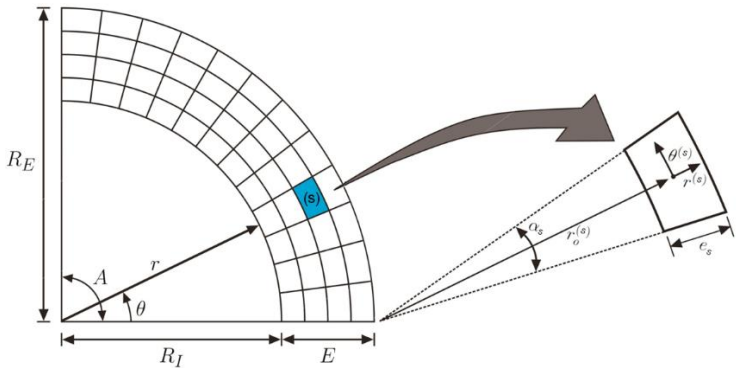


Figure 1. Domain discretized into curvilinear quadrilateral subvolumes and the local coordinate system

As in the Cartesian formulation [1], the Finite-Volume Theory for curvilinear quadrilateral subdomains,

illustrated in Fig. 1, uses a second-order polynomial in local polar coordinates to describe the temperature field in the subvolume s, as follows:

$$T^{(s)}\left(r^{(s)},\theta^{(s)}\right)=T_{(00)}^{(s)}+r^{(s)}T_{(10)}^{(s)}+\theta^{(s)}T_{(01)}^{(s)}+\frac{1}{2}\left(3\left(r^{(s)}\right)^2-\frac{e_s^2}{4}\right)T_{(20)}^{(s)}+\frac{1}{2}\left(3\left(\theta^{(s)}\right)^2-\frac{\alpha_s^2}{4}\right)T_{(02)}^{(s)} \tag{1}$$

where e_s and α_s represent the thickness and the opening angle of a subvolume, respectively, and $T_{(mn)}^{(s)}$ are unknown coefficients.

2.2 Local conductivity matrix

The surface-averaged temperatures over the curved and radial faces of a generic subvolume s in polar coordinates can be evaluated by the following expressions:

$$\bar{T}^{(s,p)}=\frac{1}{\alpha_s\left(r_o^{(s)}\mp\frac{e_s}{2}\right)}\int_{-\alpha_s/2}^{+\alpha_s/2}T^{(s)}\left(\mp e_s/2\,,\theta^{(s)}\right)\left(r_o^{(s)}\mp\frac{e_s}{2}\right)d\theta^{(s)},\ \text{for}\ p=1,3 \tag{2}$$

$$\bar{T}^{(s,p)}=\frac{1}{e_s}\int_{-e_s/2}^{+e_s/2}T^{(s)}\left(r^{(s)},\mp\alpha_s/2\right)dr^{(s)},\ \text{for}\ p=2,4 \tag{3}$$

where $\bar{T}^{(s,p)}$ denotes the surface-averaged temperature on the pth face of the subvolume s.

Applying Fourier's law in the context of polar coordinates, the heat flux density vector, $\boldsymbol{q}^{(s)}\left(r^{(s)},\theta^{(s)}\right)$, of a generic isotropic subvolume s can be expressed as:

$$\boldsymbol{q}^{(s)}\left(r^{(s)},\theta^{(s)}\right)=-\begin{bmatrix}\kappa_s & 0\\ 0 & \kappa_s\end{bmatrix}\begin{bmatrix}\partial T^{(s)}/\partial r^{(s)}\\ \left(\frac{1}{r}\right)\left(\partial T^{(s)}/\partial\theta^{(s)}\right)\end{bmatrix} \tag{4}$$

where κ_s is the thermal conductivity of subvolume s, and $r=r_0^{(s)}+r^{(s)}$ denotes the global radial coordinate.

To compute the heat exchange across subvolume boundaries in polar geometries, the normal surface-averaged heat flux densities along the faces of the subvolume must be evaluated. For the faces at constant radial positions $r=r_0^{(s)}\mp\frac{e_s}{2}$ (i.e., p = 1, 3), the surface-averaged radial heat flux density component is evaluated as:

$$\bar{q}^{(s,p)}=\mp\frac{1}{\alpha_s\left(r_o^{(s)}\mp\frac{e_s}{2}\right)}\int_{-\alpha_s/2}^{+\alpha_s/2}q_r\left(\mp e_s/2\,,\theta^{(s)}\right)\left(r_o^{(s)}\mp\frac{e_s}{2}\right)d\theta^{(s)},\ \text{for}\ p=1,3 \tag{5}$$

Similarly, for the faces located at constant angular positions $\theta=\mp\frac{\alpha_s}{2}$ (i.e., p = 2, 4), the surface-averaged circumferential heat flux density component is given by:

$$\bar{q}^{(s,p)}=\mp\frac{1}{e_s}\int_{-e_s/2}^{+e_s/2}q_\theta\left(r^{(s)},\mp\alpha_s/2\right)dr^{(s)},\ \text{for}\ p=2,4 \tag{6}$$

The local system of equations for a generic subvolume s in polar coordinates can be obtained by:

$$\bar{\boldsymbol{q}}^{(s)}=\boldsymbol{\kappa}_{(4\times4)}^{(s)}\bar{\boldsymbol{T}}^{(s)} \tag{7}$$

where $\bar{\boldsymbol{q}}^{(s)}=\left[\bar{q}^{(s,1)},\bar{q}^{(s,2)},\bar{q}^{(s,3)},\bar{q}^{(s,4)}\right]^T$ is the vector of normal surface-averaged heat flux densities, $\bar{\boldsymbol{T}}^{(s)}=\left[\bar{T}^{(s,1)},\bar{T}^{(s,2)},\bar{T}^{(s,3)},\bar{T}^{(s,4)}\right]^T$ is the vector of surface-averaged temperature and $\boldsymbol{\kappa}_{(4\times4)}^{(s)}$ is the local conductivity matrix for subvolume s.

The matrix $\boldsymbol{\kappa}_{(4\times4)}^{(s)}$ is a non-symmetric matrix, which results in increased computational cost in comparison to traditional finite element methods. Additionally, the surface-averaged temperatures are not energetically conjugated to the normal surface-averaged heat flux densities, which justifies interpreting $\boldsymbol{\kappa}_{(4\times4)}^{(s)}$ as a matrix of pseudo-conductivity matrix.

It is possible to formulate a new local system of equations which connects the surface-averaged temperatures to the normal heat fluxes on the surfaces of the subvolume s, as expressed below:

$$\boldsymbol{Q}^{(s)}=\bar{\boldsymbol{\kappa}}_{(4\times4)}^{(s)}\bar{\boldsymbol{T}}^{(s)} \tag{8}$$

where $\overline{\boldsymbol{\kappa}}^{(s)}_{(4\times4)} = \boldsymbol{L}^{(s)}\boldsymbol{\kappa}^{(s)}_{(4\times4)}$ represents the modified local thermal conductivity matrix, which is also not symmetric but relates energetically conjugated quantities, $\boldsymbol{L}^{(s)}$ represents a diagonal matrix of order 4, where the elements are the lengths of the subvolume s, given by: $L^{(s)}_{11} = \alpha_s\left(r^{(s)}_o - \frac{e_s}{2}\right)$, $L^{(s)}_{22} = e_s$, $L^{(s)}_{33} = \alpha_s\left(r^{(s)}_o + \frac{e_s}{2}\right)$ and $L^{(s)}_{44} = e_s$.

2.3 Global system assembly

The global conductivity matrix of the solid is assembled considering the individual contributions of each subvolume of the discretized domain. If the solid is subdivided in $N_s = N_\beta N_\gamma$ subvolumes, the number of faces can be evaluated as $N_f = N_\beta(N_\gamma + 1) + (N_\beta + 1)N_\gamma$. Based on the compatibility conditions for common faces, the expression that defines the global system of equations can be written as:

$$\overline{\boldsymbol{q}}_{(N_f\times1)} = \boldsymbol{\kappa}_{(N_f\times N_f)}\overline{\boldsymbol{T}}_{(N_f\times1)} \tag{9}$$

where $\overline{\mathbf{T}}_{(N_f\times1)}$ and $\overline{\mathbf{q}}_{(N_f\times1)}$ are the global surface-averaged temperature vector and the global normal surface-averaged heat flux density vector, respectively, and the global conductivity matrix can be obtained by the equation:

$$\boldsymbol{\kappa}_{(N_f\times N_f)} = \sum_{s=1}^{N_s}\left[\left(\boldsymbol{L}^{(s)}_{(4\times N_f)}\right)^T\boldsymbol{\kappa}^{(s)}_{(4\times4)}\boldsymbol{L}^{(s)}_{(4\times N_f)}\right] \tag{10}$$

where $\boldsymbol{L}^{(\mathrm{s})}_{(4\times N_f)}$ and $\left(\boldsymbol{L}^{(\mathrm{s})}_{(4\times N_f)}\right)^T$ are the temperature and normal heat flux compatibility matrices of the discretized analysis domain, respectively. The modified global system of equations can be written as:

$$\boldsymbol{Q}_{(N_f\times1)} = \overline{\boldsymbol{\kappa}}_{(N_f\times N_f)}\,\overline{\boldsymbol{T}}_{(N_f\times1)} \tag{11}$$

where $\overline{\boldsymbol{\kappa}}_{(N_f\times N_f)} = \sum_{s=1}^{N_s}\left[\left(\boldsymbol{L}^{(s)}_{(4\times N_f)}\right)^T\overline{\boldsymbol{\kappa}}^{(s)}_{(4\times4)}\boldsymbol{L}^{(s)}_{(4\times N_f)}\right]$ is the modified global conductivity matrix, obtained by summing the individual contribution of each subvolume of the discretized domain.

3 Numerical Results and Discussions

To evaluate the performance of the FVT in polar coordinates, two problems, of radial heat conduction in a thick-walled cylinder were adopted, based on a similar problem proposed by Cavalcante [9], as they possess validated analytical solutions [10, 11]. The first case considers a homogeneous metallic tube (Nickel), while the second involves a functionally graded material (FGM) tube composed of a ceramic phase (Alumina) near the inner radius and a metallic phase (Nickel) toward the outer surface. Figure 2 illustrates the cylinder, while Table 1 lists the material properties and parameters. The values were adopted to bring the cases closer to practical applications.

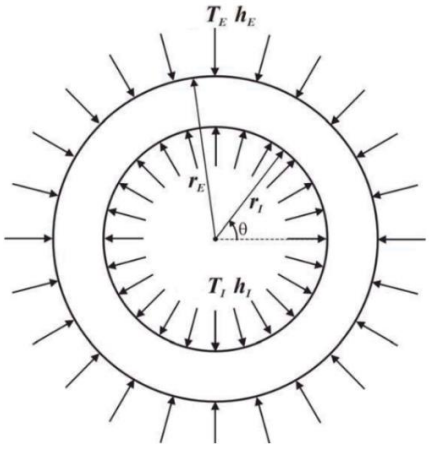


Figure 2. The thick-walled cylinder

Table 1. Material properties and adopted parameters

Material - Property	Value
Alumina - k_I	25 W· m^{-1}· K^{-1}
Nickel - k_E	60 W· m^{-1}· K^{-1}

Parameter	Value
r_E	45 mm
r_I	30 mm
T_E	20 °C
T_I	350 °C
h_E	20 W· m^{-2}· K^{-1}
h_I	1000 W· m^{-2}· K^{-1}

The inner and outer surfaces were subjected to uniform temperature boundary conditions, defined by the values T_E and h_E at the outer boundary and T_I and h_I at the inner boundary, where T and h represent the ambient temperature and the thermal convection coefficient, respectively (Fig. 2). The thermal properties were considered homogeneous and isotropic. The radial variation in conductivity for the FGM case was modeled using the expression $k(r) = k_0 r^m$, where $m = \ln(k_E/k_I) / \ln(r_E/r_I)$ and $k_0 = k_I/r_I^m = k_E/r_E^m$, ensuring that $k(r_I) = k_I$ and $k(r_E) = k_E$.

Three MATLAB® implementations were developed and analyzed. The first implementation compared FVT-Polar and analytical temperature profiles for homogeneous and FGM cases, using the solutions by Arnold *et al.* [10] (Appendix A.1) and Jabbari *et al.* [11] (Appendix A.2), respectively. In the FGM analysis, the material was modeled as a laminated medium, in which each subvolume was assigned a constant thermal conductivity equal to the value of the functionally graded material evaluated at the midpoint of the subvolume along its thickness. The numerical simulations used a mesh with 15 radial subvolumes and 1 circumferential division (15×1), solving only a 90° wedge of the cylinder due to its symmetry. The temperature values were sampled along the radial direction and plotted for comparison.

The second implementation focused on visualizing the temperature field for both material configurations in a 90° sector. A finer mesh of 15×1 subvolumes was adopted, and the center temperatures of each subvolume were used to generate contour plots, offering a qualitative assessment of the temperature distribution.

The third implementation aimed to investigate the convergence behavior of the FVT-Polar formulation by solving the same problems with varying mesh densities. The errors were evaluated by the expression, where A is the total angular extent of the domain, $T^{FVT}(r)$ and $T^{ana}(r)$ are the temperature calculated by FVT and analytical formulation, respectively.

$$Error(T) = \frac{\int_{r_I}^{r_E} |T^{FVT}(r) - T^{ana}(r)| A r dr}{\int_{r_I}^{r_E} |T^{ana}(r)| A r dr} \tag{12}$$

The subvolume thickness was progressively reduced by increasing the number of radial subdivisions (n = 3, 6, 12, 24, 48, 96). The error between both solutions was computed for each mesh, and the linear and log-log plots were generated. The slope of the log-log graph provided an estimate of the numerical convergence order.

The results of the thermal analysis are presented in Fig. 3, comparing the values obtained with the polar formulation of the FVT to the analytical solutions for both homogeneous and FGM cases.

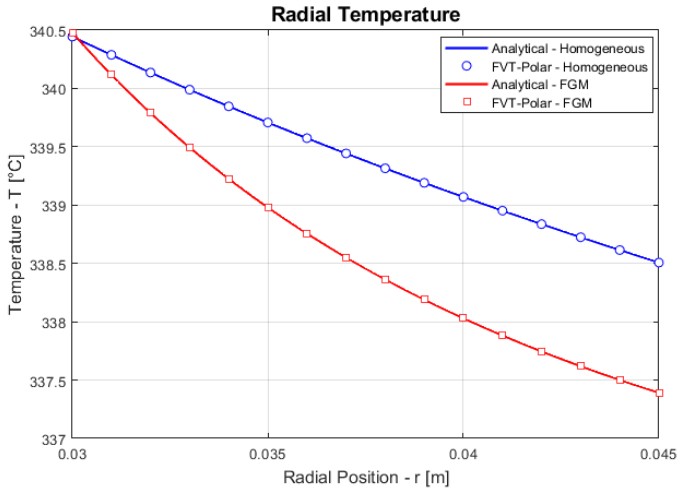


Figure 3. Temperature as a function of the radial position using the polar formulation of the FVT vs analytical solutions for both homogeneous and FGM cases.

As illustrated in Fig. 3, the radial temperature profiles for both homogeneous and functionally graded cylinders demonstrate excellent agreement between the FVT-Polar and analytical solutions, confirming the accuracy of the numerical solution. The discrete points align smoothly with the continuous curves, with no significant deviations, highlighting the effectiveness of the second-order approximation. Additionally, the use of surface-averaged quantities, rather than nodal values, contributes to the conservative nature of the solution.

The temperature fields obtained with the FVT-Polar formulation for both homogeneous and functionally graded cylinders are presented in Fig. 4.

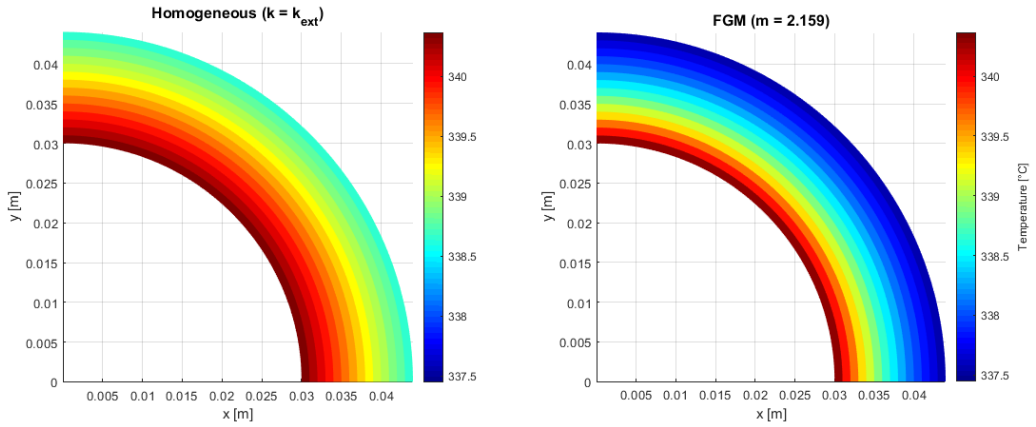


Figure 4. Temperature fields using FVT-Polar formulation for homogeneous and FGM cylinders

The solution exhibits smooth isothermal contours with no visible numerical oscillations, even with a coarse mesh of only 15 radial subvolumes. As expected, the FGM configuration results in a more intense temperature gradient near the inner surface, due to the lower thermal conductivity of the ceramic side. In contrast, the homogeneous case shows a more uniform thermal distribution throughout the domain. In both simulations, the polar discretization captures the cylindrical geometry effectively, avoiding temperature concentrations due to the staircase effect commonly observed in Cartesian grids. These results demonstrate the ability of the FVT-Polar method to provide physically consistent temperature fields even in heterogeneous materials with minimal computational effort.

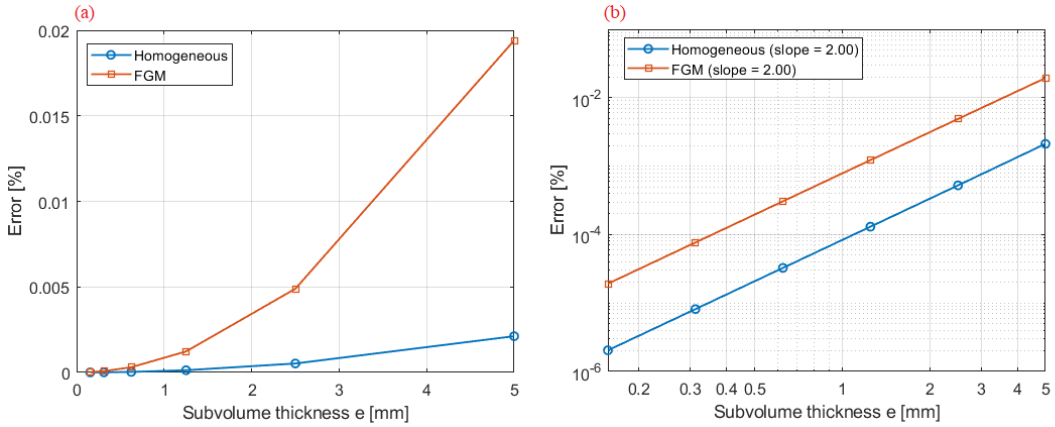


Figure 5. Convergence behavior for homogeneous and FGM cases: (a) Error (%) vs subvolume thickness (linear scale); (b) log–log plot with observed slope.

The convergence analysis is illustrated in Fig. 5, where the relative error (%) between the FVT-Polar and analytical solutions is plotted against the subvolume thickness. The error was computed using the temperature values at the mid-thickness points of each subvolume, weighted by their respective areas. Thus, instead of evaluating an integral expression for the error, a summation over all subvolumes was adopted. As shown in Fig. 5(a), the error decreases consistently with mesh refinement for both homogeneous and FGM cases. The log–log plot in Fig. 5(b) reveals a clear second-order convergence rate, with a slope of approximately 2.00 for both cases, confirming the expected efficiency of the FVT formulation. Despite the more complex conductivity profile in the FGM case, the FVT maintains its convergence behavior, highlighting its robustness. The low error magnitudes, even with coarse meshes, further reinforce the effectiveness and numerical stability of the implemented polar FVT technique.

4 Conclusions

This work presented a finite-volume formulation in polar coordinates for steady-state heat conduction in axisymmetric domains, applied to both homogeneous and functionally graded materials. The method employs second-order approximations and ensures energy conservation via surface-averaged fluxes at the faces of the subvolumes of the discretized analysis domain. The results showed excellent agreement with analytical solutions

for both cases, with smooth radial profiles and negligible deviations. Temperature maps revealed physically consistent fields with sharp radial gradients and no stress concentrations due to the staircase effect commonly observed in Cartesian grids. The convergence study confirmed a second-order convergence rate, even for spatially varying conductivity.

A key advantage of the polar formulation lies in its ability to accurately model axisymmetric problems without the need for circumferential subdivisions, reducing computational cost while preserving precision. Overall, the approach demonstrated robustness, efficiency, and high fidelity, making it suitable for thermal analysis in curved geometries and FGM structures.

Acknowledgements. The authors would like to thank the Graduate Program in Civil Engineering (PPGEC) at Federal University of Alagoas (UFAL) and the Federal Institute of Alagoas (IFAL) for institutional support, as well as the Coordination for the Improvement of Higher Education Personnel (CAPES) and the Research Support Foundation of the State of Alagoas (FAPEAL) for scholarship funding and financial support.

Authorship statement. The authors hereby confirm that they are the sole liable persons responsible for the authorship of this work, and that all material that has been herein included as part of the present paper is either the property (and authorship) of the authors, or has the permission of the owners to be included here.

Appendix

The analytical solutions proposed by Arnold *et al.* [10] for the homogeneous case and by Jabbari *et al.* [11] for the FGM case are shown below:

$$\mathrm{T(r)}_{homo} = \frac{T_I - T_E}{\ln\left(\frac{r_I}{r_E}\right) - k\left(\frac{1}{r_I h_I} + \frac{1}{r_I h_I}\right)} \ln(r) + \frac{T_I - T_E}{\ln\left(\frac{r_I}{r_E}\right) - k\left(\frac{1}{r_I h_I} + \frac{1}{r_I h_I}\right)} \left(\frac{k}{r_I h_I} - \ln(r_I)\right) + T_I \tag{A.1}$$

$$\mathrm{T(r)}_{FGM} = -\frac{A_1}{m} r^{-m} + A_2 \tag{A.2}$$

where $A_1 = \frac{h_I h_E (T_E - T_I)}{h_E (k_I r_I^{-m-1} + k_I r_I^{-m}/m) + h_I (k_E r_E^{-m-1} - k_E r_E^{-m}/m)}$ and $A_2 = \frac{h_E (k_I r_I^{-m-1} + k_I r_I^{-m}/m) T_E - h_E (k_E r_E^{-m-1} - k_E r_E^{-m}/m) T_E}{h_E (k_I r_I^{-m-1} + k_I r_I^{-m}/m) + h_I (k_E r_E^{-m-1} - k_E r_E^{-m}/m)}$

References

[1] D. T. Santos, M. A. A. Cavalcante and R. S. Escarpini Filho. "An efficient Matlab code for two-dimensional heat transfer analysis applying the finite-volume theory". In: *XLV Ibero-Latin-American Congress on Computational Methods in Engineering* (XLV CILAMCE), 2024.

[2] Y. Bansal and M. J. Pindera. "Efficient Reformulation of the Thermoelastic Higher-Order Theory for Functionally Graded Materials". *Journal of Thermal Stresses*, vol. 26, n. 11-12, pp. 1055-1092, 2003.

[3] Y. Zhong. *Efficient Reformulation of HOTFGM-Heat Conduction Case with Variable Thermal Conductivity*. M.S. Thesis, University of Virginia, 2002.

[4] Y. Zhong, Y. Bansal and M. J. Pindera. "Efficient Reformulation of the Thermal Higher-Order Theory for FGM's with Variable Thermal Conductivity". *International Journal of Computational Engineering Science*, vol. 5, n. 4, pp. 795-831, 2004.

[5] M. A. A. Cavalcante, S. P. C. Marques and M. J. Pindera. "Parametric formulation of the finite-volume theory for functionally graded materials – Part I: Analysis". *Journal of Applied Mechanics*, vol. 74, n. 5, pp. 935-945, 2007.

[6] M. A. A. Cavalcante, S. P. C. Marques and M. J. Pindera. "Parametric formulation of the finite-volume theory for functionally graded materials – Part II: Numerical Results". *Journal of Applied Mechanics*, vol. 74, n. 5, pp. 946-957, 2007.

[7] M. V. O. Araújo, E. N. Lages and M. A. A. Cavalcante. "Checkerboard-free topology optimization for compliance minimization of continuum elastic structures based on the generalized finite-volume theory". *Latin American Journal of Solids and Structures*, vol. 17, n. 8, e308, 2020.

[8] A. R. C. Santos and M. A. A. Cavalcante. "Stress analysis in axisymmetric structures using the Finite-Volume Theory formulation in polar coordinates". *Mechanics of Advanced Materials and Structures*, pp. 1-17, 2025.

[9] M. A. A. Cavalcante. *Modelling of the Transient Thermo-Mechanical Behavior of Composite Material Structures by the Finite-Volume Theory*. M.S. Thesis, Federal University of Alagoas, Maceió, Alagoas, Brazil, 2006.

[10] S. M. Arnold, B. A. Bednarcyk and J. Aboudi. "Analysis of internally cooled structures using a higher order theory". *Computers and Structures*, vol. 82, n. 7–8, pp. 659–688, 2004.

[11] M. Jabbari, S. Sohrabpour and M. Eslami. "Mechanical and thermal stresses in a functionally graded hollow cylinder due to radially symmetric loads". *International Journal of Pressure Vessels and Piping*, vol. 79, n. 7, pp. 493-497, 2002.